

## The case of 3C326: VLA 74 MHz observations during a geomagnetic storm

---

**Emanuela Orrú**

*Radboud University Nijmegen*

*Heijendaalseweg 135, 6525 AJ Nijmegen The Netherlands*

*E-mail: [e.orrui@astro.ru.nl](mailto:e.orrui@astro.ru.nl)*

**Huib Intema**

*National Radio Astronomy Observatory*

*520 Edgemont Road Charlottesville, VA 22903-2475, USA*

*E-mail: [hintema@nrao.edu](mailto:hintema@nrao.edu)*

Reaching the thermal noise at low frequencies with the next generation of instruments (e.g. SKA, LOFAR etc.) is going to be a challenge. It requires the development of more advanced techniques of calibration compared to those used from the traditional radio astronomy until now. This revolution has slowly started, from self-cal, going through field based correction and SPAM up to the formulation and application of a general Measurement Equation. We will describe and compare the several approaches of calibration used so far to reduce low frequency data. We will present some results of a 74 MHz VLA observation in exceptional ionospheric conditions of the giant radio galaxy 3C326 for which some of these methods have been successfully applied.

*ISKAF2010 Science Meeting - ISKAF2010*

*June 10-14, 2010*

*Assen, the Netherlands*



**Figure 1:** (Left) Coronal holes, (Right) sunspot and aurora pictures (center). From spaceweather.com “Another remarkable solar flare has erupted on Nov. 2nd 2003. As a result of the flare, solar protons are streaming past Earth. The ongoing radiation storm is a strong S3-class event. Passengers and crew in commercial jets at high latitudes may receive low-level radiation exposure approximately equal to one chest x-ray.”

## 1. Introduction

Spatial and temporal variations in the ionospheric free electron density can severely effect the delicate astronomical radio interferometric observations. One dominant effect is a propagation delay that depends on the ray path through the ionosphere, and therefore depends on time, the position of the interferometer elements (the antennas or stations) and the viewing direction. The free electron content of the ionosphere varies with time of day, season, geographic latitude and Solar activity. Observing with a radio interferometer in the presence of a thick ionosphere is depicted schematically in fig.2a. Here we present a VLA observation at 74 MHz of the source 3C326 obtained in extreme ionospheric conditions during a geomagnetic storm (Figure 1) for which the Source Peeling & Atmospheric Modeling (SPAM) algorithm has been applied.

## 2. The method: SPAM

Typical interferometric observations at low radio frequencies ( $<300$  MHz) require a calibration algorithm different from self-calibration, to handle direction-dependent phase errors across the field of view. Currently, only very few direction-dependent calibration algorithms exist. The SPAM algorithm (Intema et al. 2009) was developed specifically for direction-dependent ionospheric calibration and subsequent imaging. Calibration is done by ‘peeling’ available calibrators in the field of view (e.g., Nijboer & Noordam 2007), fitting a time-variant ionospheric phase screen model to the peeling phase solutions, and applying the direction-dependent model phase solutions while imaging the full field of view. For the removal of differential propagation delays, SPAM uses an ionosphere model that consists of one or several thin layers. Figure 2b sketches the model set up using one layer. This approach is successfully tested on several observations from the VLA at 74

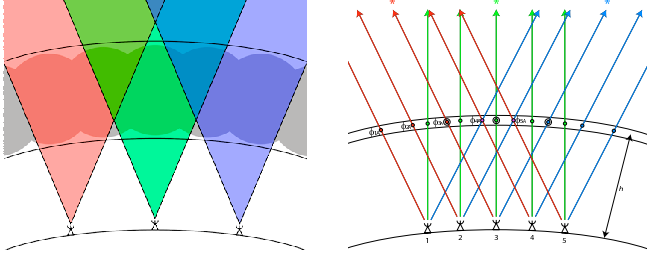


**Figure 2:** **a)** The incident extraterrestrial signals, received on each ground-based antenna, are affected by the ionosphere (grey blobs) within cone-like volumes (red, green, blue) that extends over the angular width of the field of view. The most dominant effects on radio astronomical observations are the ionosphere-induced differential propagation delays and Faraday rotations, effects that vary with time, antenna-position and viewing direction. **b)** Using calibration results towards several bright sources (red, green, blue) in the field of view, SPAM maps the calibration phases onto a fixed layer at the ionospheric pierce point positions (IPPs) of the lines-of-sight from antennas to sources. For each calibration time, SPAM fits an overall phase screen to these IPPs, using an optimized set of orthogonal base functions (van der Tol & van der Veen 2007). This model is used to interpolate the calibration phases to new IPPs along arbitrary lines-of-sight.

MHz (A&B-configurations) and the GMRT at 150 MHz. Recently, SPAM has undergone several modifications to improve convergence of the ionosphere model during more severe ionospheric conditions. These modifications include a multi-layer ionosphere model, rejection of systematically bad antennas and calibrator sources, and an FFT-based estimation of the large-scale phase gradient. This version of SPAM was used to calibrate and image the severely distorted observations of 3C326 with the VLA at 74 MHz.

### 3. Ionospheric model

As shown in fig. 3, the first part of the observation is characterized by fast phase variations, evident effect of the extreme conditions of the ionosphere. Some time ranges were too difficult to model, and were rejected during SPAM calibration.

For the peeling process we used eight bright sources found in a radius of 7.5 degrees. Thus we performed a directional calibration in 8 different patches of the field of view surrounding these sources. The central panel of fig. 4 shows the phase solutions (black dots) of the eight bright sources used for the peeling fitted with a ionospheric model (red dots) obtained by the SPAM algorithm. The model fits very well with the data for the first seven sources, while it seems to miss some features for the last one, which is the eastern lobe of 3C326. The reason of this discrepancy could be a mismatch in the assumed and true peak position of this resolved source. Note that the peeling phase solutions towards this source were excluded from the ionospheric model fit for exactly this reason. The colored panels on top and bottom of fig. 4 represent few sketches of the movie which describes the ionospheric phase variation as fitted by the model. The time resolution of each frame is 10 seconds, which corresponds to the integration time of the observation. These plots clearly show how the ionospheric phases change suddenly passing from very fine and regular patterns, in

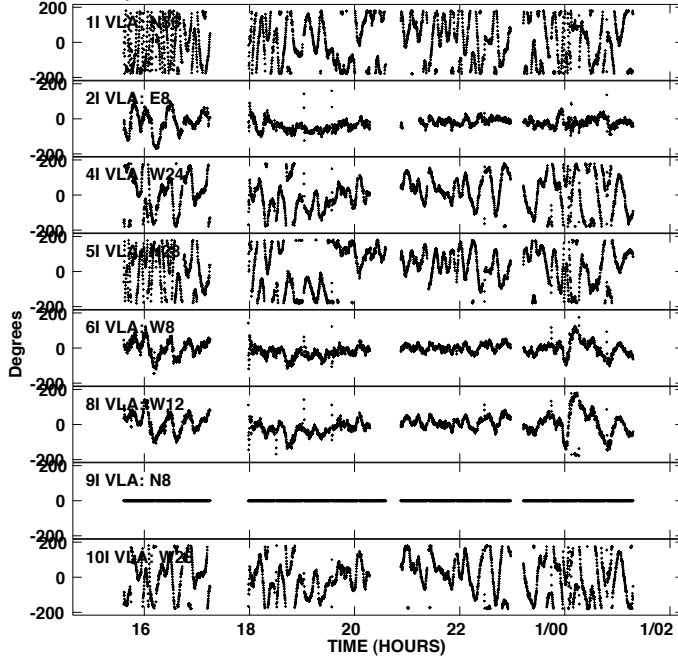


**Figure 3:** Phase solutions obtained from self-calibration.

principle easy to predict and describe with models, to wide and irregular features which complicate the calibration approach.

#### 4. SPAM versus self-calibration

Self-calibration solves for time-variable antenna phases (and amplitudes) that are assumed to be constant over the field of view. For low-frequency radio observations, the angular scale size of ionosphere-induced phase structure over each antenna is typically smaller than the field of view, thereby degrading the performance of self-calibration. In those cases, self-calibration has the tendency to find phase solutions in the direction of the field source(s) with the highest apparent flux. At larger distance from the bright source(s), the phase errors increase and source flux will be more and more scattered. This effect is demonstrated in Figure 5, which shows contour plots of the apparent field of view around 3C326 (no primary beam correction applied). The left plot and right plot were generated using self-calibration and SPAM, respectively. In comparison, the source density in the self-calibration plot drops much faster when moving away from the field center. Note that also the SPAM plot has several areas near the edges of the field that are relatively empty, like the SW region. For the latter, this could be the effect of a lack of bright-enough calibrators in that region to constrain the ionosphere model more accurately. Figure 6 shows the VLA image at 74 MHz of the source 3C326 obtained applying the SPAM algorithm.

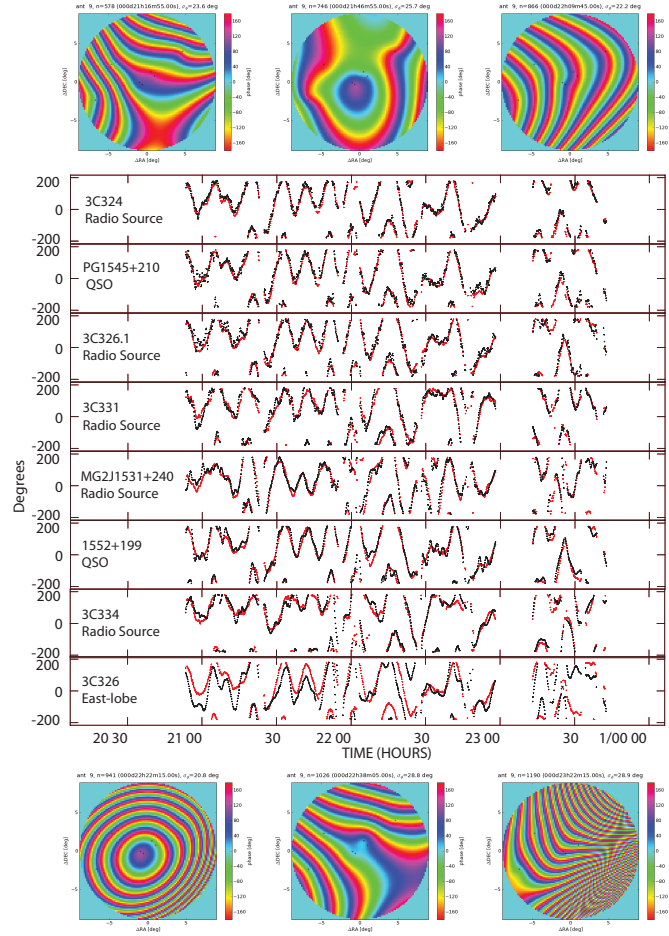


**Figure 4:** See text in ionospheric model.

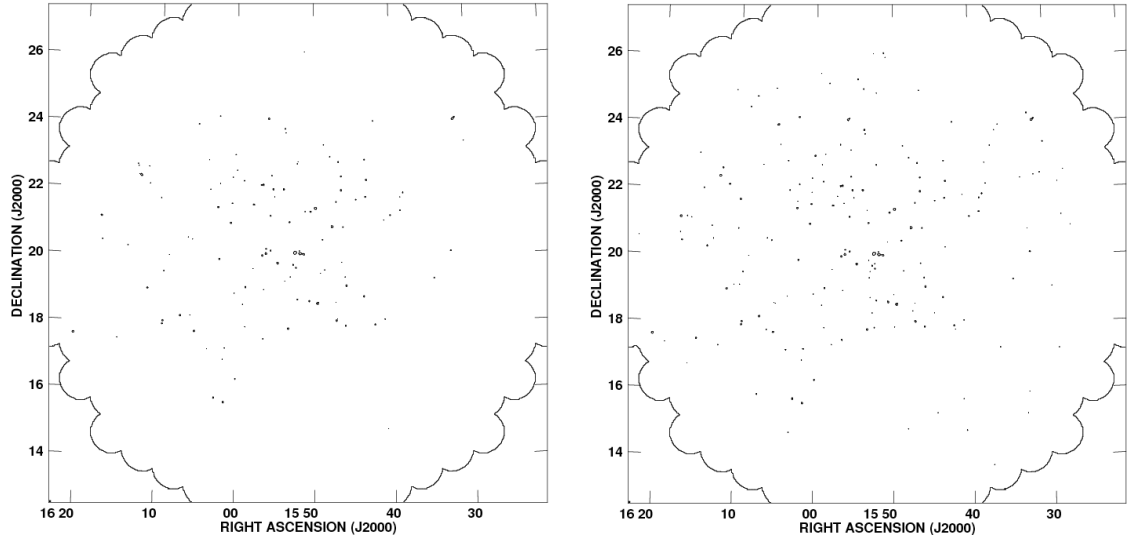


**Figure 5:** Contours of the field of view obtained with self-calibration, (Right) contours of the field of view obtained with SPAM.

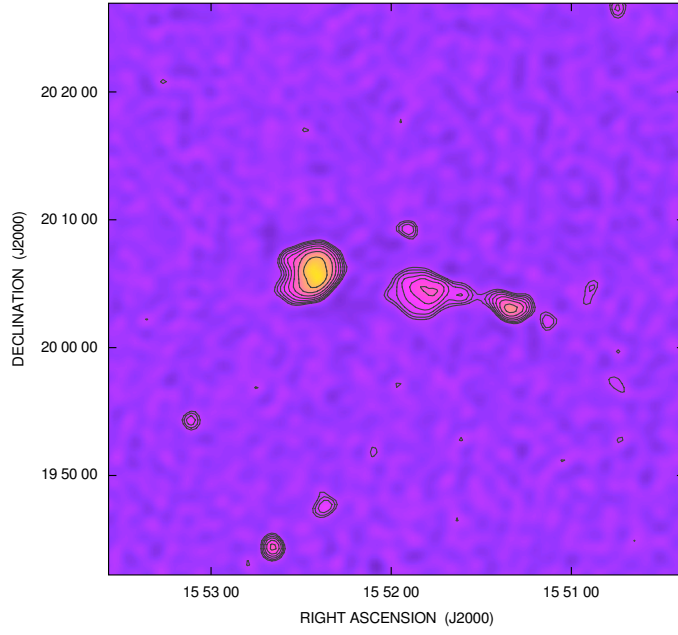


**Figure 6:** VLA image at 74 MHz of the giant radio source 3C326 obtained using the SPAM calibration method. Colors and contours show the radio brightness at 74 MHz. The rms is  $\sim 70$  mJy/beam. Contours start at  $3\sigma$  level and scale with  $\sqrt{2}$ . The resolution is  $75'' \times 75''$ .

## References

- [1] H. T. Intema, S. van der Tol, W.D. Cotton, A. S. Cohen, I. M. van Bemmelen, H. J. A. Röttgering, *A&A*, 2009, 501.1185I
- [2] S. van der Tol, B.D. Jeffs, A.-J. van der Veen, *Proceedings of the IEEE International Symposium Signals, Circuits, Systems, Iasi, Romania, 2007*, ITSP, 55.4497V
- [3] R. J. Nijboer, J. E. Noordam, *ASP Conf. Series: Astronomical Data Analysis Software and Systems* 2007, XVII 376, 237